

CHAPTER II

THEORY

2.1 Properties and characteristics of industrial catalysts

In addition to fundamental properties that come from the definition of a catalyst, such as activity, selectivity, stability, industrial applications require that a catalyst must be regenerable, reproducible, and economical as followed:

1. *Activity*: a high activity catalyst will be reflected either in high productivity from relatively small reactors and catalyst volumes or in mild operating condition, particularly temperature, which enhance selectivity and stability if the thermodynamic is more favorable.
2. *Selectivity*: High selectivity catalyst produces high yields of a desired product while suppressing undesirable competitive and consecutive reactions. This means that the texture of the catalyst (in particular pore volume and pore distribution) should be improved toward reducing limitation by internal diffusion, which in case of consecutive reactions rapidly reduces selectivity.
3. *Stability*: The catalyst with good stability will change only very slowly over the course of time under conditions of use and regeneration. Indeed, it is only in theory that a catalyst remains unaltered during reaction. Actual practice is far from this ideal. Some of the things that lead to a progressive loss of activity are as follows:
 - a) Coke forms on some catalysts through the intervention of parasitic reactions of hydrogenolysis, cyclization, and hydrogen transfer.
 - b) Reactants, products, or poisons may attack the catalyst active agents or the support.
4. *Regenerability*: As mentioned in relation to stability, it is only in theory that the catalyst is found intact at the end of the reaction. All catalysts age; and when their activities or their selectivity have become insufficient, they must be regenerated through a treatment that will return part or all of their catalytic properties. The most common treatment is burning off of carbon, but scrubbing with suitable gases is also frequently done to desorb certain reversible poisons; hydrogenolysis of hydrocarbon compounds may be done when the catalyst permits it, as well as an injection of

chemical compounds. When the treatment does not include burning off carbon deposits, it is often called rejuvenation.

5. *Reproducibility*: Reproducibility characterizes the preparation of a catalyst as much as the catalyst itself; it is of concern to industrial users who want to be assured of the quality of successive charges of catalyst

6. *Cost*: Even when catalyst possesses all the properties and characteristics just enumerated, these remain one last requirement: it must withstand comparison with competitive catalysts or processes with equivalent functions from the point of view of cost; or at least its cost should not place too heavy a burden on the economics of the process for which it will be used.

Table 2.1 A roster of catalyst by order of increasing acid activity as obtain for isomerisation, polymerization and cracking [22]

Acid catalyst (by increasing activity)	Isomerisation of <i>n</i> -C5	Polymerization of C ₃ H ₆ at 200°C	Cracking of <i>n</i> -C ₇ H ₁₆ (temp. in 10% conversion)
alpha-alumina	inactive	0	inactive
silica	inactive	0	inactive
TiO ₂	inactive	0	inactive
low surface Al ₂ O ₃	500°C	<1%	inactive
high surface Al ₂ O ₃	450°C	0-5%	490°C
fluorinated-alumina	380°C	>80%	420°C
silica-alumina	360°C	>90%	410°C
exchanged zeolite	260°C	>95%	350°C
AlCl ₃ /Al ₂ O ₃	120°C	100%	100°C

From Table 2.1, besides AlCl₃, the exchanged zeolite exhibits a higher activity in every process due to its higher acidity; however, zeolites play an important role in product selectivity more than AlCl₃.

2.2 Zeolite molecular sieves

Molecular sieves are porous materials that exhibit selective adsorption properties which can be classified on the IUPAC definitions into three main types depending on their pore sizes that are microporous materials, mesoporous materials, and macroporous materials. Properties and examples of these materials are shown in Table 2.2.

Table 2.2 IUPAC Classification of porous materials

Type of materials	Pore size (Å)	Examples
Microporous materials	< 20	zeolites, activated carbon
Mesoporous materials	20 – 500	M41s, SBA-15, pillared clays
Macroporous materials	> 500	glasses

Zeolites, a type of molecular sieves, are crystalline aluminosilicates of alkali and alkaline earth metals. They both occurred in nature and archived from synthesis. The unique properties of zeolites i.e. high surface area, high sorption, ion exchange, and high acidity have been exploited for their catalytic applications such as oil refining (as cracking catalysts and as adsorbents), petrochemical industry, and synthesis of chemicals.

2.2.1 Basic units of zeolites

A zeolite has a three dimensional network structure of tetrahedral primary building units (PBU) which made of four oxygen anions with either silicon $[\text{SiO}_4]$ or aluminum cation $[\text{AlO}_4]^-$ in the center as shown in Figure 2.1(a). Then, a secondary building unit (SBU) consists of selected geometric groupings of those tetrahedra by sharing oxygen atom as shown in Figure 2.1(b).

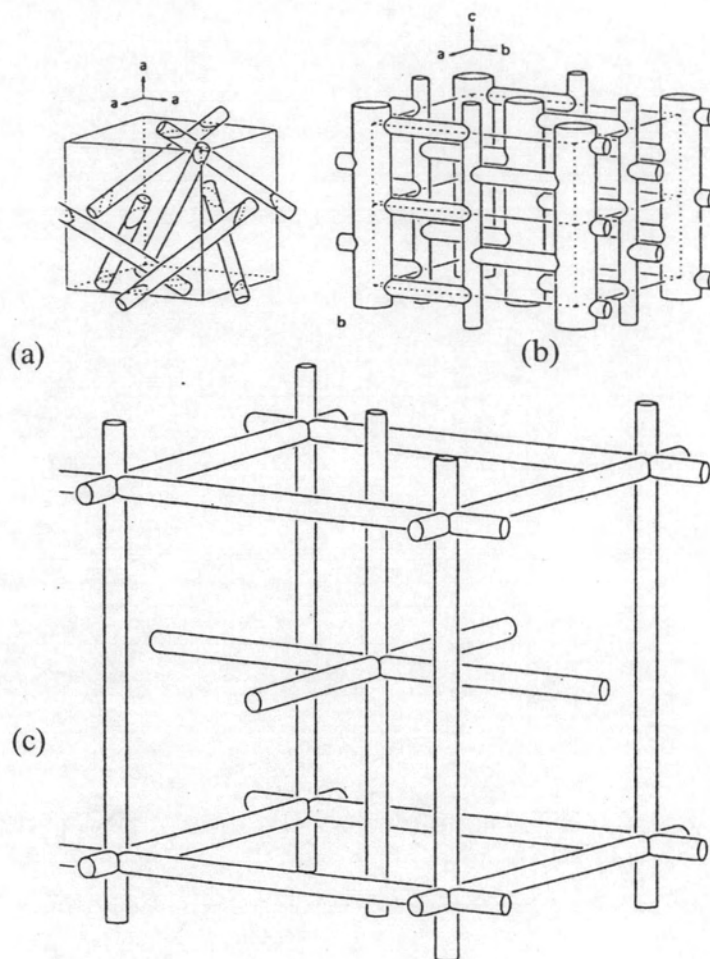


Figure 2.2 Three types of channel in zeolites (a) one-dimension system represented in analcime, (b) two-dimension system of mordenite structure, and (c) three-dimension system of paulingite [23].

1. One-dimension system: The channels do not intersect together that is found in analcime as shown in Figure 2.2 (a)
2. Two-dimension system: The main parallel channels are crossed by perpendicular channel but between sheets are not linked such as mordenite.
3. Three-dimension system: This system can be divided into two types. The former, the channel are equidimensional, the diameters of all channels are equal, regardless of direction. The latter consists of three-dimension intersecting channels, but the channels are not equidimensional. The diameter depends upon the crystallographic direction.

2.2.3 Properties of zeolites

2.2.3.1 Shape and size selectivity

The zeolites ability to preferentially sieve molecules can be used in many useful ways. If a reactant is sterically unable to enter the zeolite pores, where the reaction takes place, then the product resulting from that reactant is also restricted (Figure 2.3). In the second case, if a product forms inside the zeolitic cavity but is unable to leave, again it is restricted (Figure 2.4).

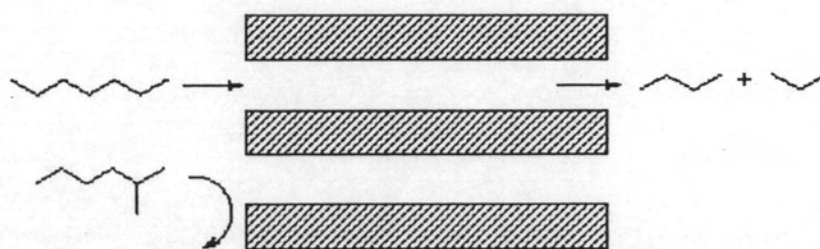


Figure 2.3 Schematic diagram of reactant shape selectivity: rejection of branched chain hydrocarbons.

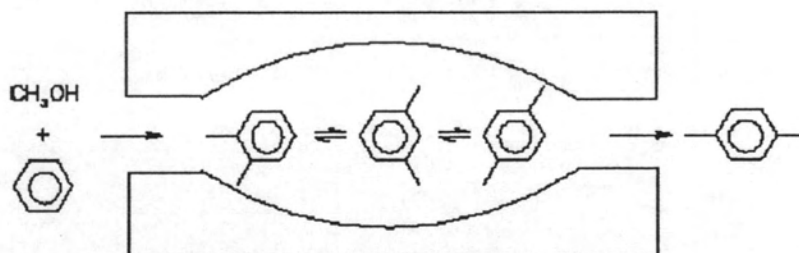


Figure 2.4 Schematic diagram of product shape selectivity: p-xylene diffuses preferentially out of the zeolite channels.

2.2.3.2 Acidity of zeolites

In addition to shape and size selective catalysis, the generation of acidic sites within the zeolite pores gives rise to a highly efficient solid acid catalysis. The isomorphous replacement of silicon with aluminum in a tetrahedra site gives rise to a charge imbalance because aluminum has lower coordination ability than silicon and must be neutralized.

This is achieved in two ways in natural zeolites:

- The Al-O bond length becomes slightly longer.
- A coordination site is made available for cation to counter the excess negative charge.

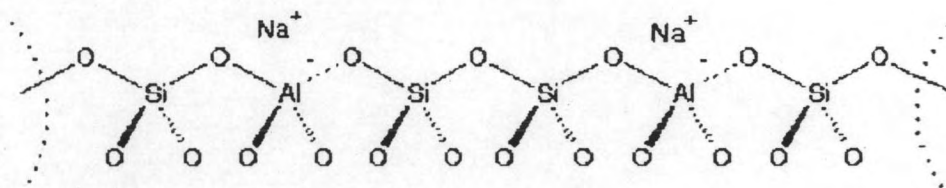


Figure 2.5 Sodium balanced zeolite framework [24].

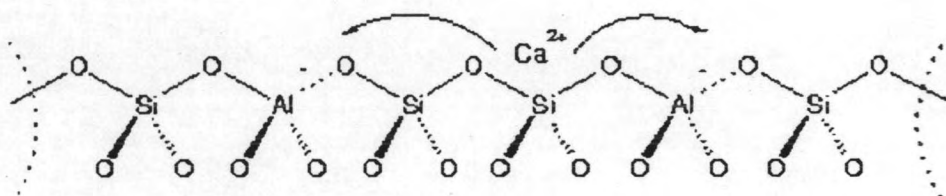


Figure 2.6 Calcium balanced zeolite framework [24].

In natural zeolites, the excess negative charge is balanced by whatever ions are present in the surrounding environment e.g. K^+ , Na^+ , Mg^{2+} and Ca^{2+} as exhibited in Figure 2.5 and Figure 2.6. The type of counter ion used to balance the charge plays an important part in the use of the zeolite. This cannot be any clearer than on replacement of the cation with a proton by hydrothermal treatment to form a hydroxyl group at the oxygen bridge. The acid site formed behaves as a classic Brønsted, proton donating acid site as shown in Figure 2.7.

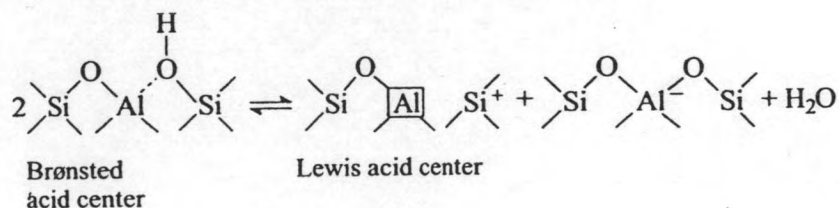


Figure 2.7 Brønsted and Lewis acid site in zeolites [25].

The highly acidic sites, combined with the high selectivity arising from shape selectivity and large internal surface area makes the zeolite an ideal industrial catalyst. The significance of this acidic proton can be shown quite easily by comparisons of experiments in H^+ -exchanged zeolites and their equivalent cation form zeolite. For example, the MTG process is highly dependent on the presence of the Brønsted proton, if the catalytic H-ZSM-5 is replaced by the purely siliceous analogue of ZSM-5 which has no Brønsted protons, the reaction does not take place at all. Therefore, the modification of zeolite structure can be increase their activity, which are very economically important step for industry.

2.3 Mesoporous materials

Mesoporous materials are a type of molecular sieves, such as silicas or transitional aluminas or modified layered materials such as pillared clays and silicates. Mesoporous silica has uniform pore sizes from 2 to 50 nm and has found great utility as catalysts and sorption media because of the regular arrays of uniform channels. Larger surface area is desired for enhancing of the reactions.

2.3.1 Classification of mesoporous materials

Mesoporous materials can be classified by different synthetic procedures into three categories as described in Table 2.3.

Table 2.3 Classification of mesoporous materials by synthesis procedure

Assembly	Template	Media	Material
(a) Electrostatic	quaternary ammonium salt	base or acid	MCM-41
(b) H-bonding	primary amine	neutral	HMS
(c) H-bonding	amphiphilic triblock copolymer	acid (pH<2)	SBA-15

2.3.2 Synthesis strategies of mesoporous materials

Crystalline molecular sieves are generally obtained by hydrothermal crystallization. The reaction gel, usually, contains cation (e.g. Si^{4+} for silicate materials, Al^{3+} for aluminate materials) to form the framework; anionic species (e.g. OH^- and F^-); organic template and solvent (generally water). Typically, the nature of

template can be considered into two parts that are hydrophobic tail on the alkyl chain side and hydrophilic head on the other side. The examples of template used are primary, secondary tertiary and quaternary amines, alcohols, crown or linear ethers, and as well as polymer. An understanding of how organic molecules interact with each other and with the inorganic frameworks would increase the ability to design rational routes to molecular sieve materials. The organic templates are frequently occluded in the pores of the synthesized material, contributing to the stability of mineral backbone.

2.3.2.1 The behavior of surfactant molecules in an aqueous solution

In a simple binary system of water-surfactant, surfactant molecules, at a particular concentration can aggregate to form micelles in various types. The shapes of micelle strongly depend on the concentrations as shown in Figure 2.8.

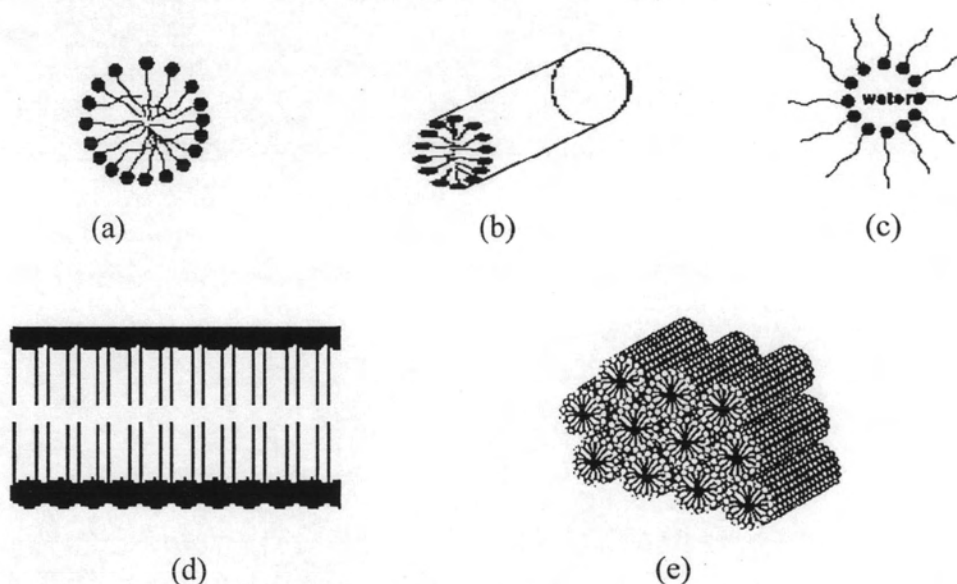


Figure 2.8 Phase sequence of the surfactant-water binary system (a) spherical micelle, (b) rod-shaped micelle, (c) reverse micelle, (d) lamellar phase, and (e) hexagonal phase.

At low concentration, they energetically exist as isolated molecules. With increasing concentration, surfactant aggregate together to form isotropic spherical and rod shaped micelles by directing the hydrophobic tails inside and turning the hydrophilic heads outside in order to decrease the system entropy. The initial

concentration threshold at which those molecules aggregate to form isotropic micelle is called critical micelle concentration (CMC). The CMC determines thermodynamic stability of the micelles. When the concentration is continuously increased, the micellar shape changes from sphere or rod shape to hexagonal, lamellar, and inverse micelles. The particular phase present in a surfactant aqueous solution depends not only on the concentrations but also on the nature of surfactant molecules such as its length of the hydrophobic carbon chain, hydrophilic head group, and counter ion. Moreover the ionic strength, pH value, and temperature including other additives are the factors determining the shape of micelles.

2.3.2.2 Interaction between inorganic species and surfactant micelles

The major components of framework structure, mainly silicate, present in aqueous solution as inorganic species. To acquire the desired structure, firstly the template forms the proper shape, and then the inorganic soluble species interact with the surfactant as shown in Table 2.4. The hybrid solids formed are strongly dependent on the interaction between surfactants and the inorganic precursors.

Table 2.4 Example routes for interactions between the surfactant and the inorganic soluble species

Surfactant type	Inorganic type	Interaction type	example materials
Cationic (S^+)	I^-	S^+I^-	MCM-41, MCM-48
	I^+X^-	$S^+X^-I^+$	SBA-1, SBA-2, zinc phosphate
	I^0F^-	$S^+F^-I^0$	silica
Anionic (S^-)	I^+	S^-I^+	Al, Mg, Mn, Ga
	IM^+	$S^-M^+I^-$	alumina, zinc oxide,
Neutral S^0 or N^0	I^0	S^0I^0 or N^0I^0	HMS, MSU-X, aluminum oxide
	I^+X^-	$S^0X^-I^+$	SBA-15

Where S^x or N^x : surfactant with charge of X

I^x : inorganic species with charge of X

X^- : halogenide anions

F^- : fluoride anion

M^{n+} : with charge of X

In case of ionic surfactant (S^+ and S^-), the hydrophilic head mainly binds with inorganic species through electrostatic interactions. There are two possible formation routes. Firstly, direct pathway: surfactant and inorganic species of which charges are opposite interact together directly (S^+I^- and S^-I^+). Another is the indirect pathway, occurring when the charges of surfactant and inorganic species are the same, so the counter ions in solution get involved as charge compensating species for example the $S^+X^-I^+$ path takes place under acidic conditions, in the presence of halogenide anions ($X^- = Cl^-$ or Br^-) and the $S^-M^+I^-$ route is the characteristic of basic media, in the existence of alkaline cation ($M^+ = Na^+$ or K^+). Figure 2.9 shows the possible hybrid inorganic-organic interfaces.

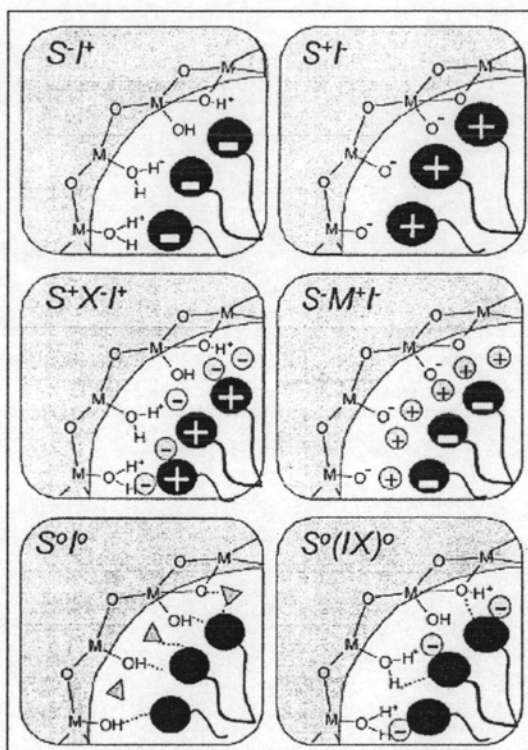


Figure 2.9 Schematic representation of the different types of silica-surfactant interfaces. Dashed line corresponded to H-bonding interactions [26].

Using non-ionic surfactant (S^0 or N^0), the main interaction between template and inorganic species is hydrogen bonding or dipolar, which is called neutral path i.e. S^0I^0 and $S^0F^-I^+$. Nowadays, non-ionic surfactants give important commercial advantages in comparison to ionic surfactants because they are easily removable, nontoxic, biodegradable and relatively cheap.

2.3.2.3 Formation mechanism of mesoporous materials

Mechanism of mesoporous formation can be classified on the basis of synthetic route into three types exhibited in Figure 2.10:

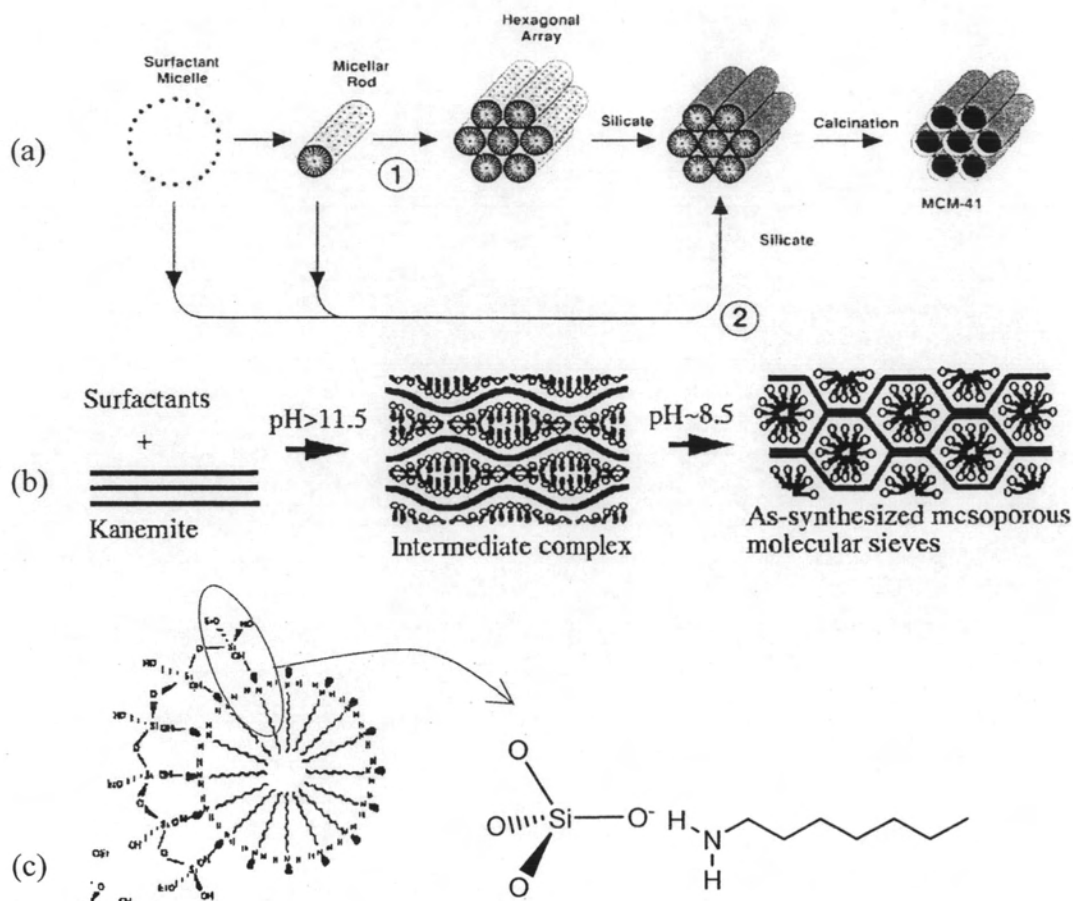


Figure 2.10 Mechanism of mesoporous formation (a) LCT of MCM-41 formation, (b) Folding sheet formation of FSM-16 and (c) H-bonding interaction in HMS formation [9, 27].

(a) *Liquid crystal Templating mechanism*: i.e. MCM-41. From Figure 2.10(a) there are two main pathways; firstly, liquid crystal phase was intact before silicate species were added or another pathway is the addition of the silicate results in the ordering of the subsequent silicate-encased surfactant micelles.

(b) *Folding sheet formation*: i.e. FSM-16. The intercalation of ammonium surfactant into hydrate sodium silicate, which composes of single layered silica sheets called “kanemite” (ideal composition $\text{NaHSi}_2\text{O}_5 \cdot 3\text{H}_2\text{O}$), produced the lamellar-to-hexagonal phase in FSM-16. After the surfactants were ion exchanged into layered

structure, the silicate sheets were thought to fold around the surfactants and condense into a hexagonal structure.

(c) *Hydrogen-bonding interaction*: The neutral templating produced mesoporous materials with thicker walls and higher thermal stability as compared to the LCT-derived silicates.

Although some of mesoporous as described above have the same hexagonal structure, they are different in the properties as shown in Table 2.5. Since the thermal and hydrothermal stability of material are based on the wall thickness, therefore, from Table 2.5 SBA-15 possesses and exhibits significantly higher thermal and hydrothermal stability than other materials. Furthermore, its pore size can be expanding up to 300 Å which allow the bulky molecule to diffuse into their pores.

Table 2.5 Properties of some hexagonal mesoporous materials

Material	Pore size (Å)	Wall thickness (nm)	BET specific surface area (m ² /g)
MCM-41	15-100	1	>1000
HMS	29-41	1-2	640-1000
FSM-16	50-300	no report	680-1000
SBA-15	15-32	3-6	630-1000

2.3.3 Synthesis strategy of mesoporous material using block-copolymer as structure directing agent

In the synthesis of mesoporous materials such as MCM-41, FSM-16 ionic surfactant i.e. the cationic, alkyltrimethyl ammonium (C_nTA^+ , $8 < n < 18$), and anionic surfactant, tertiary amine ($C_nH_{2n+1}N^+(CH_3)_3$) are used as template, respectively. These syntheses were done in extreme (alkaline) pH condition and the obtained materials having pore size in the range of 15 to 100 Å only. However, by this mean, two limitations occurred:

- (1) The lower stability of the obtained materials: due to the thinner pore wall of materials (8-13 Å).

- (2) Difficult to expand the pore size: the ionic surfactants give a limited pore size. The only way to expand the pore size is in employing swelling agents such as 1,3,5-trimethyl benzene, involving complicate synthesis.

Thus, the block copolymer has been used to solve these problems. Generally, amphiphilic block copolymer has been used in the field of surfactants, detergent manufacturing, emulsifying, coating, etc. The properties of block copolymer can be continuously tuned by adjusting solvent composition, molecular weight, or type of polymers. Figure 2.11 shows typical block copolymer used as templates.

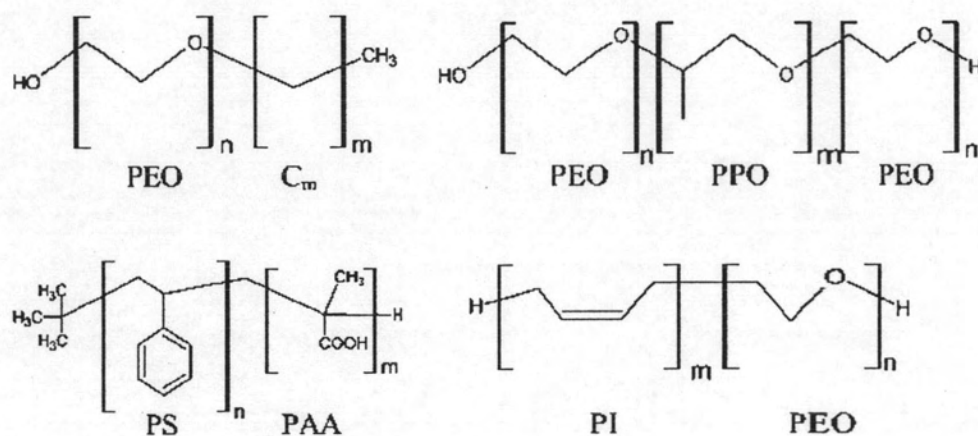


Figure 2.11 Block copolymer used in mesostructured generation [28].

Some advantages of using these block copolymer are:

- (1) *The thicker wall thickness* (about 15-40 Å), enhancing hydrothermal and thermal stability of materials.
- (2) *Pore diameter can be tuned easier* by varying type or concentration of polymer.
- (3) *Easier to remove from mineral framework* by thermal treatment or solvent extraction. Due to the hydrogen bonding interaction between template and inorganic framework, therefore, it should be easier to dissociate as compared to ionic templates (electrostatic interaction).

Interaction between block copolymer template and inorganic species, called hybrid interphase (HI), is particularly important, especially in PEO-PPO based one.

one. Different possible interactions taking place at the HI are schematized in Figure 2.12. Most of the fine HI characterization has been performed on PEO-based (di or triblock) templates. Melosh *et al.* [28] determined that in F127-templated silica monoliths, organization arose for polymer weight fractions higher than 40%. For lower polymeric/silica ratios, non-ordered gels were formed. This lack of order was due to a relatively strong interaction (probably of H-bonding type) of the (Si—O—Si) polymers forming the inorganic skeleton with both PEO and PPO blocks.

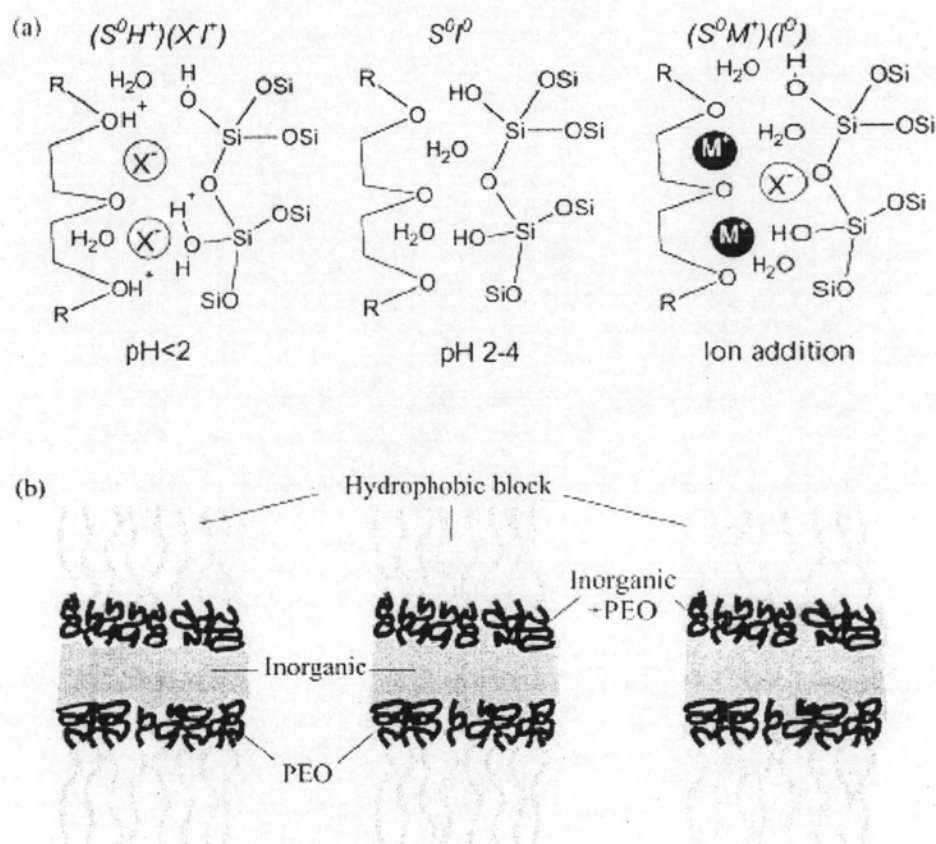


Figure 2.12 (a) Schematic view of the $(S^0H^+)(X^-)$, S^0P^0 , and $(S^0M^+)(P^0)$ hybrid interphases (HIs) (b) Three possible structures of a HI composed by a nonionic polymer and an inorganic framework [29].

2.4 SBA-15

2.4.1 Structure and properties of SBA-15

Recently, SBA-15 mesoporous material has been synthesized under acidic condition using triblock copolymer as a structure directing agent. This novel mesoporous material has shown higher hydrothermal stability as compared to MCM-41 due to its thicker pore walls (3.1-6.4 nm). They also possess uniform and hexagonal-structured channels similar to MCM-41 as shown in Figure 2.14 with larger pore size which make them more desirable to deal with bulky molecule. Some properties of MCM-41 and SBA-15, two well-known materials, are compared as described in Table 2.6. According to the properties listed in Table 2.6 SBA-15 show a better performance than MCM-41 in almost of properties.

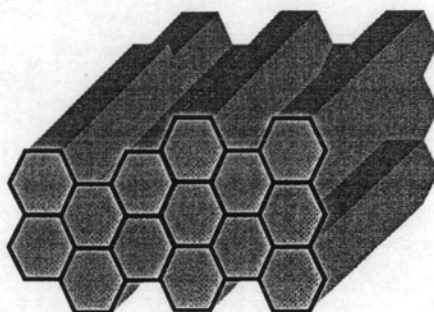


Figure 2.13 Hexagonal mesoporous structure.

Table 2.6 Comparison of two well-known mesoporous materials, MCM-41 and SBA-15 in their characteristic properties [7, 10]

Properties	MCM-41	SBA-15
pore size (Å)	20-100	46-300
pore volume (ml/g)	>0.7	0.8-1.23
surface area (m ² /g)	>1000	690-1040
wall thickness (Å)	10-15	31-64

2.4.2 Synthesis of SBA-15 and formation mechanism

For SBA-15 materials, aging time and temperature are particularly important. Kruk *et al.* found that mesoporous SBA-15 prepared from calcination of an 'as-prepared' hybrid precursor contained a significant fraction of microporosity; further aging of the precursor in the mother liquors leads to an improvement on the

pore size distribution (Figure 2.15), in agreement with the first work by Zhao *et al.* [10].

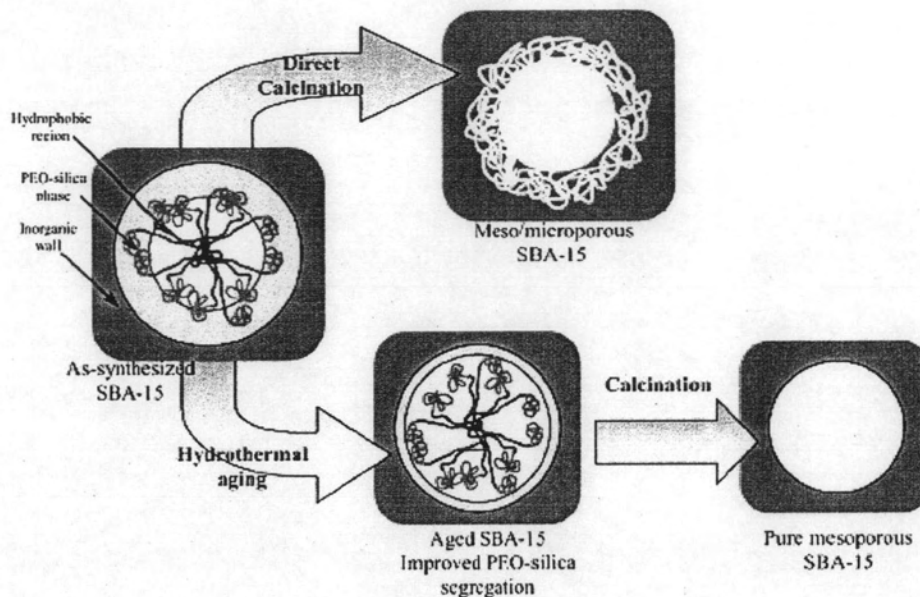
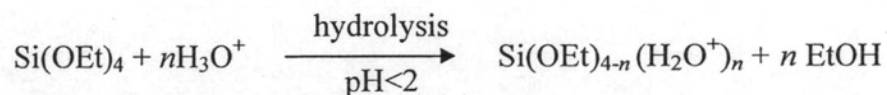


Figure 2.14 Pore evolution upon thermal treatment, depending on pre-treatment and aging [29].

Aging of an as-prepared precipitate at 80–100 °C seems to help segregation of the PEO blocks and the inorganic framework, by promoting condensation of the latter. High temperatures also change the polymer behavior. It is known that for $T > 60$ °C, PEO blocks become less hydrophilic and expel water (the same is valid for the more hydrophobic PPO blocks, for $T > 40$ °C) [29]. For a mechanism, firstly alkoxy silane species (TMOS or TEOS) are hydrolyzed as:



which is followed by partial oligomerization at the silica. Furthermore, at this condition, the PEO parts of surfactant associate with hydronium ions as followed:



Next, coordination sphere expansion around the silicon atom by anion coordination of the form $X^-SiO_2^+$ may play an important role. The hydrophilic PEO blocks are expected to interact with the protonated silica and thus be closely associated with the inorganic wall. During the hydrolysis and condensation of the silica species, intermediate mesophase is sometimes observed and further condensation of silica species and organization of the surfactant and inorganic species result in the formation of the lowest energy silica-surfactant mesophase structure allowed by solidifying network.

2.4.3 Incorporation of aluminum into SBA-15

Among the metal-substituted mesoporous materials, aluminum-incorporated mesoporous materials have great potential in moderating acid-catalyzed reactions for large molecules. However, it is very difficult to introduce the metal ions directly into SBA-15 due to the easy dissociation of metal-O-Si bonds under strong acidic conditions.

2.4.3.1 Direct synthesis

To date, only a few studies on the direct synthesis of Al-SBA-15 have been reported [16-18]. The comparison of direct and post synthesis of Al-SBA-15 are described in Table 2.7.

Table 2.7 Comparison of direct synthesis and post synthesis method of Al-SBA-15 [16-20]

	Direct synthesis method	Post synthesis method
<i>Synthesis condition</i>	Require complicated procedure	Simply method
<i>Aluminum form in materials</i>	Most of sample have both tetrahedral and octahedral aluminum	Most of sample have only tetrahedral aluminum
<i>Catalyst activity</i>	Lesser activity due to extra-framework aluminum	Higher activity due to aluminum in framework

As knowing from Section 1.2.2 (The development of synthesizing Al-SBA-15), many literatures were claimed that the direct synthesis of Al-SBA-15 is difficult and often not stoichiometric.

From this viewpoint, therefore, the development of a simple post-synthesis method for the alumination of the mesoporous silicas that are synthesized under strongly acidic conditions becomes an appealing alternate choice.

2.4.3.2 Post synthesis

Nowadays, several post synthesis method where aluminum was grafted onto the mesoporous wall with various aluminum sources such as $\text{Al}(\text{CH}_3)_3$, AlCl_3 have been developed without the mesoporous structure seriously destroyed [19]. In the case of zeolites, the introduction of Al into their framework will lead to the formation of bridging hydroxyl groups (Brønsted acid sites). However, whether the similar situation occurs in mesoporous materials still keeps argument. Some researchers assigned the hydroxyl vibration at about 3606 cm^{-1} in IR spectrum to the acidic bridging hydroxyl groups while others disagree the assignment. For example, Trombetta *et al.* argued that the Brønsted acid sites in mesoporous materials or aluminosilicates resulted from terminal silanol groups in the vicinity of aluminum atoms [30]. After the adsorption of a basic probe, such as pivalonitrile, the terminal silanol groups were induced to form the bridging hydroxyl groups (SiOHAl , shown in Figure 2.15).

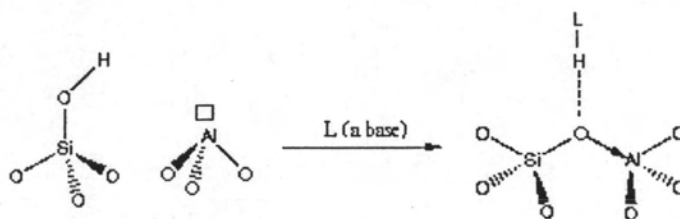


Figure 2.15 Alumination of mesoporous material using basic probe (L) inducing to form the bridging hydroxyl group [17].

2.5 Characterization of mesoporous hexagonal structure

2.5.1 Powder x-ray diffraction (XRD) [31]

X-ray powder diffraction (XRD) is a reliable technique that can be used to identify mesoporous structure. Typically, the XRD pattern of hexagonal symmetry show five well-resolved peaks that can be indexed to the corresponding lattice planes of Miller indices (100), (110), (200), (210), and (300). These XRD peaks appear at small angle (2θ angle between 2 and 5 degree) due to the materials are not crystalline at atomic level, diffraction at higher angles are not observed.

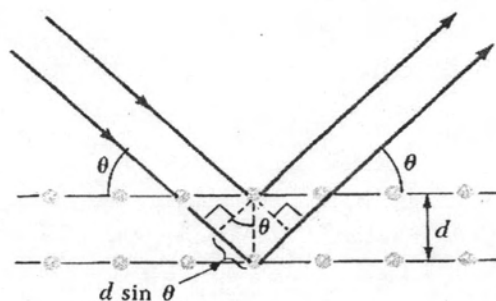


Figure 2.16 Diffraction of X-ray by regular planes of atoms.

Figure 2.16 shows a monochromatic beam of X-ray incident on the surface of crystal at an angle, θ . The scattered intensity can be measured as a function of scattering angle 2θ . The resulting XRD pattern efficiently determines the different phases present in the sample structure. Using this method, Bragg's law is able to determine the interplanar spacing of the samples, from diffraction peak according to Bragg's angle.

$$n\lambda = 2d \sin\theta$$

Where the integer n is the order of the diffracted beam, λ is the wavelength; d is the interplanar distance of the crystal (the d -spacings) and θ is the angle of between the incident beam and these planes.




2.5.2 Inductively coupled plasma – atomic emission spectroscopy (ICP-AES) [22]

It is essential to determine elemental composition to be assured that the composition of active elements in catalyst is close to what expected. It is also often used in explanation of the life time of catalyst by using the elemental composition of

catalyst. To do these, chemical methods of analysis such as ICP-AES, XRF are still in use. Table 2.8 has shown physical methods of analysis for catalytic elements.

Table 2.8 Physical method of analysis for catalytic elements

1 H Hydrogen 1.00784																	2 He Helium 4.003
3 Li Lithium 6.941	4 Be Beryllium 9.012											5 B Boron 10.811	6 C Carbon 12.011	7 N Nitrogen 14.006	8 O Oxygen 15.999	9 F Fluorine 18.998	10 Ne Neon 20.180
11 Na Sodium 22.990	12 Mg Magnesium 24.305											13 Al Aluminum 26.982	14 Si Silicon 28.086	15 P Phosphorus 30.974	16 S Sulfur 32.06	17 Cl Chlorine 35.453	18 Ar Argon 39.948
19 K Potassium 39.098	20 Ca Calcium 40.078	21 Sc Scandium 44.956	22 Ti Titanium 47.88	23 V Vanadium 50.942	24 Cr Chromium 51.996	25 Mn Manganese 54.938	26 Fe Iron 55.845	27 Co Cobalt 58.933	28 Ni Nickel 58.69	29 Cu Copper 63.546	30 Zn Zinc 65.38	31 Ga Gallium 69.723	32 Ge Germanium 72.64	33 As Arsenic 74.922	34 Se Selenium 78.96	35 Br Bromine 79.904	36 Kr Krypton 83.80
37 Rb Rubidium 85.468	38 Sr Strontium 87.62	39 Y Yttrium 88.906	40 Zr Zirconium 91.224	41 Nb Niobium 92.906	42 Mo Molybdenum 95.94	43 Tc Technetium 98	44 Ru Ruthenium 101.07	45 Rh Rhodium 102.905	46 Pd Palladium 106.36	47 Ag Silver 107.868	48 Cd Cadmium 112.411	49 In Indium 114.818	50 Sn Tin 118.710	51 Sb Antimony 121.757	52 Te Tellurium 127.6	53 I Iodine 126.905	54 Xe Xenon 131.29
55 Cs Cesium 132.905	56 Ba Barium 137.327	57 La Lanthanum 138.905	58 Ce Cerium 140.12	59 Pr Praseodymium 140.908	60 Nd Neodymium 144.24	61 Pm Promethium 145	62 Sm Samarium 150.36	63 Eu Europium 151.964	64 Gd Gadolinium 157.25	65 Tb Terbium 158.925	66 Dy Dysprosium 162.50	67 Ho Holmium 164.930	68 Er Erbium 167.259	69 Tm Thulium 168.934	70 Yb Ytterbium 173.054	71 Lu Lutetium 174.967	
87 Fr Francium [223]	88 Ra Radium [226]	89 Ac Actinium [227]	104 Rf Rutherfordium [261]	105 Db Dubnium [262]	106 Sg Seaborgium [263]	107 Bh Bohrium [264]	108 Hs Hassium [265]	109 Mt Meitnerium [266]	110	111	112	113	114				
58 Ce Cerium 140.12	59 Pr Praseodymium 140.908	60 Nd Neodymium 144.24	61 Pm Promethium [145]	62 Sm Samarium 150.36	63 Eu Europium 151.964	64 Gd Gadolinium 157.25	65 Tb Terbium 158.925	66 Dy Dysprosium 162.50	67 Ho Holmium 164.930	68 Er Erbium 167.259	69 Tm Thulium 168.934	70 Yb Ytterbium 173.054	71 Lu Lutetium 174.967				
90 Th Thorium [232]	91 Pa Protactinium [231]	92 U Uranium [238]	93 Np Neptunium [237]	94 Pu Plutonium [244]	95 Am Americium [243]	96 Cm Curium [247]	97 Bk Berkelium [247]	98 Cf Californium [251]	99 Es Einsteinium [252]	100 Fm Fermium [257]	101 Md Mendelevium [258]	102 No Nobelium [259]	103 Lr Lawrencium [262]				

 analyzed by atomic absorption
  analyzed by flame spectrometry
  analyzed by both methods

2.5.3 Solid state ^{27}Al -nuclear magnetic resonance [23, 32]

Since 1980, NMR has established itself as a major and unique analytical tool in the characterization on the structural features of solid materials including zeolites and other aluminosilicates. Table 2.9 shows the relevant nuclei, the directly relevant nuclei in zeolite studies has been ^{29}Si and ^{27}Al -NMR which provide framework or structural information about zeolite or mesoporous molecular sieves.

Table 2.9 NMR properties of selected nuclei

Isotope	Spin	Natural abundance (%)
^1H	1/2	99.98
^{23}Na	3/2	100
^{27}Al	5/2	100
^{29}Si	1/2	4.70
^{129}Xe	1/2	26.44
^{205}Tl	1/2	70.50

An advantage in examining ^{27}Al -NMR spectra is that ^{27}Al has a 100 percent natural abundance with $I = 5/2$ and ranges in chemical shift about 450 ppm. Quadrupole coupling must be separated from chemical shift effect to render useful chemical information from ^{27}Al -NMR spectrum. For the low Si/Al molar ratios where the Si (Al) resonance is very weak in the ^{29}Si -NMR spectra, incorporation of Al in the framework can readily be demonstrated via ^{27}Al -NMR. The ^{27}Al -NMR has been used mainly for the detection of extra-framework aluminum, since the ^{27}Al -NMR chemical shifts depend primarily on the coordination of aluminum with respect to oxygen. For tetrahedral coordination, chemical shifts of 55 to 80 ppm from $\text{Al}(\text{H}_2\text{O})_6^{3+}$ are observed. Octahedral Al appears at 0 to 22 ppm. Both the solid and solution spectra show similar ranges. The position of the signal in ^{27}Al -NMR spectra is also sensitive to the composition of material, i.e. the nature of counter ion, degree of hydration of sample. In dehydrated sample, quadrupolar effects are so strong that the tetrahedral Al line disappears, reappearing on dehydration. No effect is observed for the octahedrally bound aluminum with changing degrees of hydration.

2.5.4 Temperature-programmed desorption of ammonia [23]

Temperature-Programmed Desorption of Ammonia (NH_3 -TPD) is the most widely used method to measure the acidic property of solid in mesoporous materials. On widely various solid acid catalysts, it was clarified that desorption was controlled by the equilibrium between the gaseous and adsorbed ammonia under usually utilized experimental conditions. There are many variations on the method, but it typically involves saturation of the surface with ammonia under some set of adsorption conditions, followed by linear ramping of the temperature of the sample in a flowing inert gas stream. The amount of ammonia desorbing above some characteristic temperature is taken as the acid-site concentration, and the peaks desorption temperature (T_M) have been used to calculate heats of adsorption. It is well known that desorption temperature of the ammonia molecule can be related to the strength of acidity of the materials tested. The bond formed between the acid site and the ammonia is broken by an energy supply. Thus, the maximum temperature in the NH_3 desorption process is a qualitative indication of the strength of the acid sites.

2.5.5 Nitrogen adsorption-desorption technique [33, 34]

The N₂ adsorption-desorption technique is used to determine the physical properties of mesoporous molecular sieves, that are surface area, pore volume, pore diameter and pore-size distribution of solid catalysts. Adsorption of gas by a porous material is described by an adsorption isotherm, the amount of adsorbed gas by the material at a fixed temperature as a function of pressure. Porous materials are frequently characterized in terms of pore sizes derived from gas sorption data. The IUPAC classification of adsorption isotherms is illustrated in Figure 2.17.

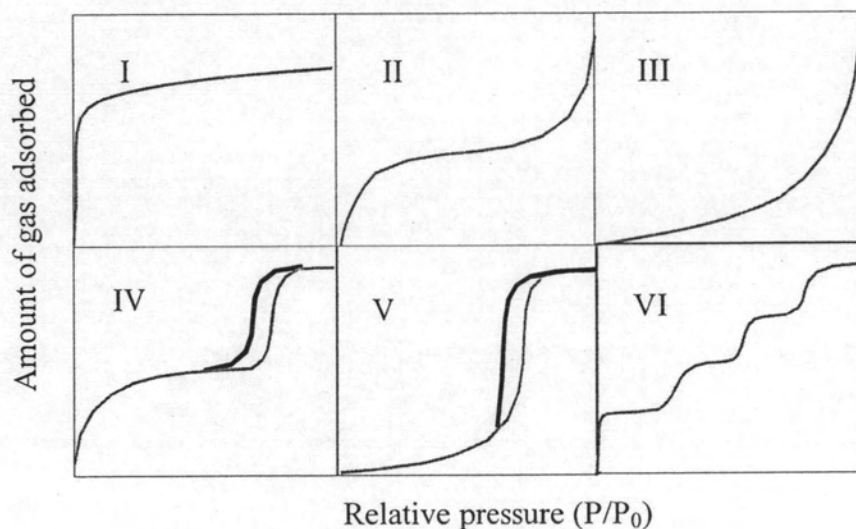


Figure 2.17 The IUPAC classification of adsorption isotherm.

Adsorption isotherms are described as shown in Table 2.10 based on the strength of the interaction between the sample surface and adsorptive. Pore size distribution is measured by the use of nitrogen adsorption/desorption isotherm at liquid nitrogen temperature and relative pressures (P/P_0) ranging from 0.05-0.1. The large uptake of nitrogen at low P/P_0 indicates filling of the micropores (<20 Å) in the adsorbent. The linear portion of the curve represents multilayer adsorption of nitrogen on the surface of the sample, and the concave upward portion of the curve represents filling of mesoporous and macropores. The multipoint Brunauer, Emmett and Teller (BET) method is commonly used to measure total surface area.

$$\frac{1}{W[(P_0/P)-1]} = \frac{1}{W_m C} + \frac{C-1}{W_m C} (P/P_0)$$

where W is the weight of nitrogen adsorbed at a given P/P_0 , and W_m is the weight of gas to give monolayer coverage, and C is a constant that is related to the heat of adsorption. A slope and intercept are used to determine the quantity of nitrogen adsorbed in the monolayer and calculate the surface area. For a single point method, the intercept is taken as zero or a small positive value, and the slope from the BET plot is used to calculate the surface area. The surface area reported depend upon the method used, as well as the partial pressures at which the data are collected.

Table 2.10 Features of adsorption isotherms

Type	Interaction between sample surface and gas adsorbate	Porosity	Example of sample-adsorbate
I	relatively strong	Micropores	activated carbon-N ₂
II	relatively strong	Non porous	oxide-N ₂
III	weak	Non porous	carbon-water vapor
IV	relatively strong	Mesopore	silica-N ₂
V	weak	Micropores	activated carbon-water vapor
		Mesopore	
VI	relatively strong sample surface has an even distribution of energy	Nonporous	graphite-Kr

2.5.6 Scanning electron microscope [35]

The scanning electron microscope (SEM) has unique capabilities for analyzing surfaces and morphology of materials. It is analogous to the optical microscope, although different radiation sources serve to produce the required illumination. Whereas the optical microscope forms an image from light reflected from a sample surface, the SEM uses electrons for image formation. The different wavelength of these radiation sources result in different resolution levels: electron have much shorter wavelength than light photons, and shorter wavelength are capable of generating the higher resolution information. Enhanced resolution in turn permits higher magnification without loss of detail. The maximum magnification of the light

microscope is about 2,000 times; beyond this level is “empty magnification”, or the point where increased magnification does not provide additional information. This upper magnification limit is a function of the wavelength of visible light, 2000 Å, which equal the theoretical maximum resolution of conventional light microscope. In comparison, the wavelength of electron is less than 0.5 Å, and theoretically the maximum magnification of electron beam instrument is beyond 800,000 times. Because of instrumental parameters, practical magnification and resolution limits are about 75,000 times and 40 Å in a conventional SEM. The SEM consists basically of four systems:

1. The *illuminating/imaging system* produces the electron beam and directs it onto the sample.
2. The *information system* includes the data released by the sample during electron bombardment and detectors which discriminate among analyze these information signals.
3. The *display system* consists of one or two cathode-ray tubes for observing and photographing the surface of interest.
4. The *vacuum system* removes gases from the microscope column which increase the mean free path of electron, hence the better image quality.

2.6 Cracking reaction

Cracking is the name given to breaking up large hydrocarbon molecules (lower value stock) into smaller and more useful bits (light and middle distillate). This is achieved by using high pressures and temperatures without a catalyst (thermal cracking or pyrolysis), or lower temperatures and pressures in the presence of a catalyst (catalytic cracking). In refinery, the source of the large hydrocarbon molecules is often the naphtha fraction or the gas oil fraction from the fractional distillation of crude oil (petroleum). These fractions are obtained from the distillation process as liquids, but are re-vaporized before cracking. There is not any single unique reaction happening in the cracker. Any acid would do, but in a conventional chemical reaction of hydrocarbons with a strong acid (e.g., H_2SO_4), it would be kind of difficult both to separate out what we wanted afterward and avoid corroding cracking reactors. Thus, the catalysts used are solids with acidic surfaces, so they stay where they are put. A major difference between thermal cracking and catalytic

cracking is that reaction through catalytic cracking occurred via carbocation intermediate, compared to the free radical intermediate in thermal cracking as shown in Figure 2.18. Carbocation has longer life and accordingly more selective than free radicals, therefore, the catalytic cracking product can be controlled more easily than those of thermal cracking.

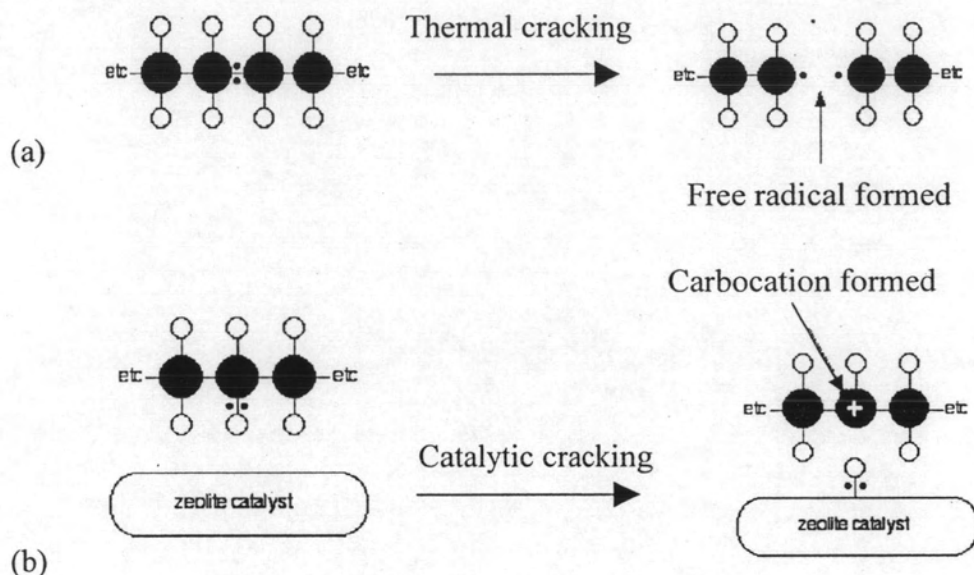
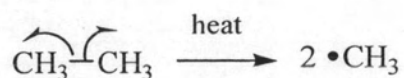


Figure 2.18 Model for cracking of hydrocarbon via (a) thermal cracking and (b) catalytic cracking.

2.6.1 Thermal cracking [36]

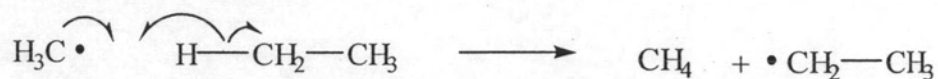
In thermal cracking, high temperatures (typically in the range of 450 to 750°C) and pressures (up to 70 atm) are used in breaking the large hydrocarbons into smaller ones. The mechanism in thermal cracking began when the initiating radicals are formed by spontaneous bond rupture. For example, in case of ethane cracking, there are only two types of bonds that can be broken i.e. the C-C bond and the C-H bonds. The bond dissociation energies of the C-C bond requires somewhat less energy. Hence, fragmentation of a few ethane molecules into two methyl radicals takes place.

First initiation step:



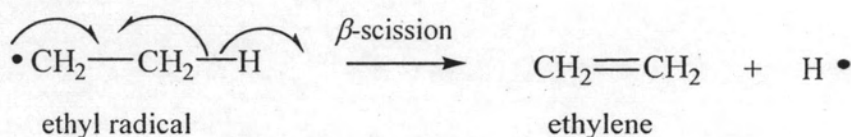
In a second initiation step, a methyl radical abstracts a hydrogen atom from another ethane molecule:

Second initiation step:

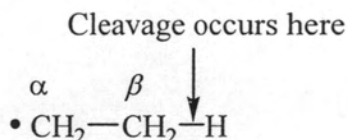


This step accounts for small amounts of methane formed in the cracking process. The ethyl radical is the chain-propagating radical. It first undergoes an interesting reaction in which it “unzips” to yield ethylene and a hydrogen atom in a process called β -scission:

First propagation step:

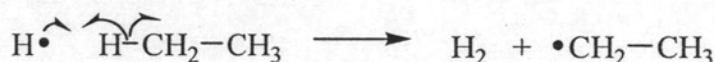


β -scission is another typical reaction of free radicals. The word “scission” means “cleavage”. Beta position (β) refers to the fact that the cleavage occurs one carbon away from the radical site.



The hydrogen atom produced in the first propagation step then abstracts a hydrogen atom from another molecule of ethane to give a new ethyl radical:

Second propagation step:



The ethyl radical then enters into the first propagation reaction, thus continuing the free-radical chain. The hydrogen that is a by-product of second propagation step is collected and may be used to produce ammonia by hydrogenation of nitrogen in

refinery. It can be seen that there are four types of reactions that free radicals can undergo. Three of these are reactions that produce other radicals:

1. Addition to a double bond
2. Atom abstraction
3. β -Scission.

The other reaction eliminates free radicals:

4. Recombination of two free radicals to form a covalent bond.

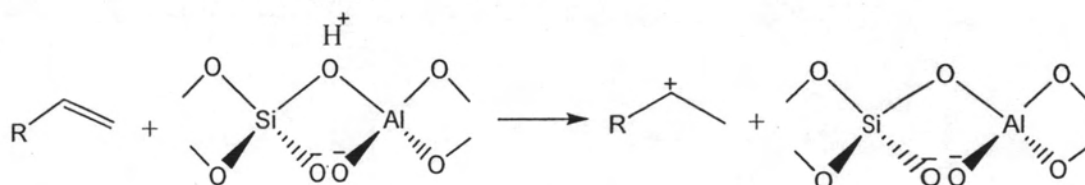
2.6.2 Catalytic cracking [6]

In catalytic cracking, the following illustrates the different ways by which carbocations may be generated in the reactor:

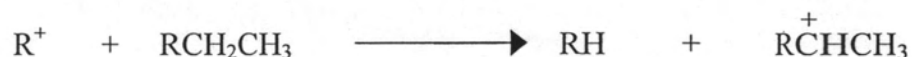
1. Abstraction of a hydride ion by a Lewis acid site from a hydrocarbon



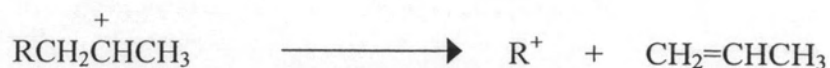
2. Reaction between a Brønsted acid site (H^+) and an olefin



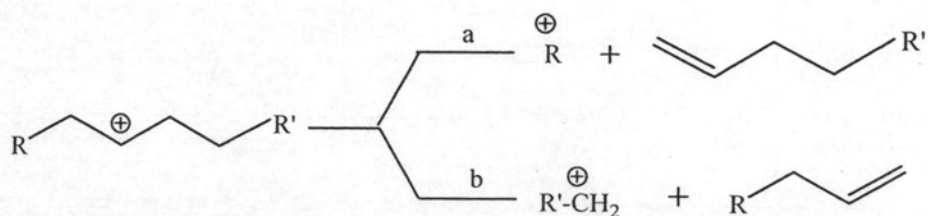
3. Reaction of a carbonium ion formed from step 1 or 2 with another hydrocarbon by abstraction of hydride ion



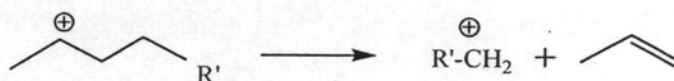
Abstraction of hydride ion from a tertiary carbon is easier than from secondary, which is easier than from a primary position. The form of carbocation can rearrange through a methide-hydried shift. This isomerisation reaction is responsible for a high ratio of branched isomers in the products. The most important cracking reaction is the carbon-carbon beta bond scission. A bond at a position beta to the positively-charged carbon breaks heterolytically, yielding an olefin and another carbocation. This can be represented by the following example:



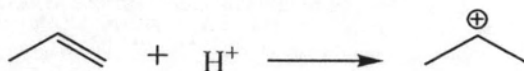
A new carbocation may experience another beta scission, rearrange to a more stable carbonium ion or react with a hydrocarbon molecule in the mixture and produced paraffin. The carbon-carbon beta scission may occur on either side of the carbocation, with the smallest fragment usually containing at least three carbon atoms. For example, cracking a secondary carbocation formed from a long chain paraffin could be represented as followed:



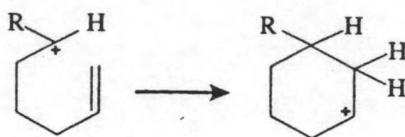
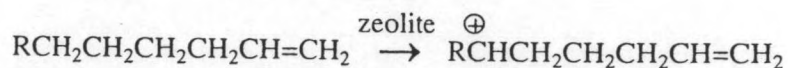
If $\text{R}=\text{H}$ in the above example, then according to the beta scission rule, only route (b) becomes possible, and propylene would be a product:



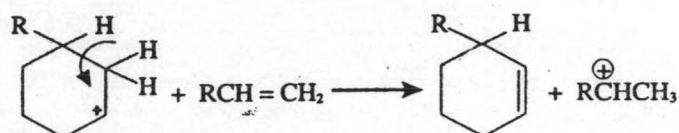
The propene may be protonated to an isopropyl carbocation:



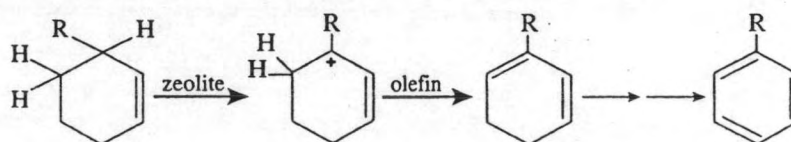
An isopropyl carbocation cannot experience beta fission (no C-C beta bond to the carbon with positive charge). It may either abstract a hydride ion from another hydrocarbon, yielding propane, or revert back to propene by eliminating a proton. This could explain the relatively higher yield of propene from catalytic cracking units than from thermal cracking units. Aromatization of paraffins can occurred through a dehydrocyclization reaction. Olefinic compounds formed by beta scission can form a carbocation intermediate with the configuration conducive to cyclization. For example, if a carbocation such as that shown below is formed (by any of the methods mentioned earlier), cyclization is likely to occur.



Once cyclization has occurred, the formed carbocation can lose a proton, and a cyclohexene derivative is obtained. This reaction is aided by the presence of an olefin in the vicinity ($\text{R}-\text{CH}=\text{CH}_2$)



The next step is the abstraction of a hydride ion by a Lewis acid site from the catalyst surface to form the more stable allylic carbocation. This is again followed by a proton elimination to form a cyclohexadiene intermediate. The same sequence is followed until the ring is completely aromatized.



During the cracking process, fragmentation of complex polynuclear cyclic compounds may occur, leading to formation of simple cycloparafins. These compounds can be a source of C_6 , C_7 , and C_8 aromatics through isomerisation and hydrogen transfer reactions. Coke formed on the catalyst is thought to be due to polycondensation of aromatic nuclei. The reaction can also occur through a carbonium ion intermediate of benzene ring. The polynuclear aromatic structure has a high C/H ratio.